

Determination of the deuterium plasma density ratio \hat{n}_d/\hat{n}_e through neutron measurements

To cite this article: O.N. Jarvis *et al* 1987 *Nucl. Fusion* **27** 1755

View the [article online](#) for updates and enhancements.

Related content

- [Determination of deuterium concentrations in JET plasmas](#)
O.N. Jarvis, J.M. Adams, B. Balet *et al.*
- [Neutron measurement techniques for tokamak plasmas](#)
O N Jarvis
- [Prediction/modelling of the neutron emission from JET discharges](#)
O N Jarvis and S Conroy

Recent citations

- [Time-dependent neutron-rate interpretation for neutral-beam-heated tokamak plasmas](#)
B Wolle *et al*
- [Neutron measurement techniques for tokamak plasmas](#)
O N Jarvis
- [Neutron Spectroscopy with a \$^3\text{He}\$ Ionization Chamber on TFTR](#)
Takeo Nishitani and J. D. Strachan



IOP | ebooks™

Bringing together innovative digital publishing with leading authors from the global scientific community.

Start exploring the collection—download the first chapter of every title for free.

DETERMINATION OF THE DEUTERIUM PLASMA DENSITY RATIO \hat{n}_d/\hat{n}_e THROUGH NEUTRON MEASUREMENTS

O.N. JARVIS, G. GORINI, J. KÄLLNE,
V. MERLO, G. SADLER, P. VAN BELLE
JET Joint Undertaking,
Abingdon, Oxfordshire,
United Kingdom

ABSTRACT. JET has been operating with deuterium plasmas for the past two years, during which time neutron spectrometry has been applied as a diagnostic technique for determining the ion temperature for suitable discharges. Combining the 'neutron temperature' with the neutron yield determination made with a fission counter diagnostic permits the central deuterium to electron density ratio (\hat{n}_d/\hat{n}_e) to be determined. It is found that this ratio, for ohmically heated discharges, appears to fall with ion temperature from about 70% at 2 keV to 40% at 3 keV. The addition of ICRF heating does not alter the density ratio. These findings are consistent with the observation that high temperatures achieved with Ohmic heating in tokamaks are correlated with high impurity levels.

1. INTRODUCTION

Two neutron diagnostic systems are used on the JET tokamak, one for the measurement of the fusion reaction rate and the other for measuring the central ion temperature for deuterium plasma discharges under conditions of Ohmic heating, supplemented (perhaps) with ICRF additional heating with H or ^3He minority ions. Under such conditions the deuterium ions are expected to be in thermal equilibrium, an assumption which is necessary for the discussion presented below.

The first of the diagnostic systems involves the measurement of the yield of neutrons from the $d + d \rightarrow n + ^3\text{He}$ reaction and, in some form or other, is a standard measurement for all levels of neutron emission on tokamaks world wide. The second diagnostic, involving ion temperature measurements with a neutron spectrometer on a per discharge basis, is unique to JET but nonetheless is restricted to high neutron yield discharges ($>10^{12}$ neutrons emitted per second).

As is well-known, the total neutron emission rate is given by

$$Y_n \sim \int n_d^2 \langle \sigma v \rangle d^3x$$

where the integral is taken over the whole plasma volume. The reactivity, $\langle \sigma v \rangle$, is strongly temperature dependent, varying as T_i^α , where $\alpha \sim 4$ at $T_i = 3$ keV.

The neutron diagnostics independently determine both Y_n and \bar{T}_i . If it can be assumed that the radial dependences of the deuterium ion density and temperature are the same as those measured for electrons – which, whilst not strictly correct, should be an acceptable approximation – then the remaining unknown quantity, the central deuterium ion density \hat{n}_d , can be determined. For convenience, we express this quantity in ratio form as a density ratio \hat{n}_d/\hat{n}_e . It is, of course, assumed that the density and temperature profiles rise to a peak in the centre of the magnetic flux surfaces, at a radius of about 3.05 m.

2. FUSION REACTION RATE MEASUREMENTS

The 2.5 MeV neutrons emitted in one of the two branches of the d–d fusion reaction are recorded with three pairs of ^{235}U and ^{238}U fission chambers supported from the vertical limbs of the poloidal field magnet yoke at the level of the horizontal midplane. Neutrons emitted from the plasma discharge are essentially confined by the massive structure surrounding the vacuum vessel, and those which escape must do so through one of the several openings, of which the horizontal diagnostic ports are the largest. Some of these escaping neutrons will scatter from the port windows into the direction of the fission chambers.

The ^{235}U fission chambers, employing polyethylene moderator and substantial lead shielding, have been

designed to give a fairly flat response with neutron energy [1]. The fission chamber response of the neutron emitting volume element in the plasma varies considerably with position around the torus. Accordingly, this variation has been measured [2] with the aid of ^{252}Cf radioisotope and 14 MeV pulsed tube neutron sources placed inside the JET vacuum vessel. With this information, the quantitative relationship between the neutron emission from a plasma discharge (for which the relevant plasma parameters are known) and the response of the fission chamber has been determined to a precision of $\pm 10\%$ at a neutron flux level corresponding to a total source strength of 10^8 neutrons \cdot s $^{-1}$. The fission chambers are operated in both pulse counting and current sampling modes but for the work reported here the flux level remained within the operational range of the pulse counting mode so that response linearity need not be questioned.

3. NEUTRON SPECTROMETRY

The neutron spectrometer used in this work was a Jordan Valley type FNS-1 ^3He ionization chamber located in the Roof Laboratory at JET so as to view the centre of the plasma at a distance of 20 m vertically below. The shielding was excellent but the collimation was necessarily severe so that only the most intense of ohmically heated discharges provided useful neutron fluences. Further details of the experimental arrangement and examples of the measured energy spectra are given in Ref. [3].

The neutron energy spectrum from a plasma in thermal equilibrium is very nearly Gaussian in form, with a width which gives the ion temperature directly, through the relationship [4] $\text{fwhm} = 82.5\sqrt{\bar{T}_i}$, with fwhm and \bar{T}_i in keV. The recorded energy spectrum is representative of a line integral through the plasma, albeit heavily weighted to the plasma core. The resultant energy spectrum remains Gaussian but is somewhat narrowed. The correction [5] to be applied to the line averaged \bar{T}_i to obtain the central value \hat{T}_i is 1.09 ± 0.01 for radial dependences of T_i and n_d described by peaking factors (see later) lying in the range $\pm 50\%$ about their nominal values.

The experimental pulse height spectra are, of course, rather broader than the neutron energy spectra because of the finite resolution of the ^3He spectrometer itself. The spectrometer response function for monoenergetic neutrons takes the form of a narrow (40 keV fwhm) Gaussian full energy peak with a small amplitude (5%) tail extending to low energies which is attributed to a

detector wall effect. The experimental pulse height spectra have been fitted [5], by using a maximum likelihood method, to curves generated from the convolution of the measured response function and a pure Gaussian, with Gaussian fwhm and amplitude as the only significant variables. A correlated error analysis is performed to obtain the uncertainty in the fwhm and, therefore, in \hat{T}_i .

The analysed pulse height distributions have all been fitted successfully with no significant deviations from Poisson statistics being observed. Because of the low energy tail to the response function [5], about 700 counts in the full energy peak are required to give a 10% accuracy in \hat{T}_i . To obtain this count, it was frequently necessary to perform a sum over repeated, 'identical', discharges. Discharges for which the neutron fluence was insufficient to provide better than 25% statistical accuracy (<100 counts) were not analysed since it is rare that discharges are repeated more than a few times without altering plasma conditions. In addition to the purely statistical uncertainty, there is also a systematic uncertainty related to the particular choice of spectrometer response function. This was assumed to be energy independent in view of the very narrow neutron energy range explored (2.45 ± 0.15 MeV). The systematic uncertainty in \hat{T}_i is estimated to be $\pm 5\%$ and is not temperature dependent.

4. ION TEMPERATURE DATA

Over the two years during which JET has been operating with deuterium plasmas, there have been only about 50 Ohmic and ICRF heated discharges of sufficient neutron emission intensity and plasma current flat-top duration to warrant analysis of the neutron spectrometer pulse height data. As is shown in Table I, most of these discharges provided statistical uncertainties in \hat{T}_i which are in excess of 15% but, since several similar discharges were run consecutively, it was possible to improve the accuracy by aggregating the data. In some instances the plasma discharges were intentionally not quite identical so that wherever feasible the data were analysed on a single discharge basis and derived quantities such as \hat{n}_d/\hat{n}_e were averaged afterwards. Of course, the averaged \hat{T}_i for a group of discharges was always independent of whether individual results were averaged or all the spectra were summed and a single averaged temperature derived. The averaged plasma parameters for each group of discharges are presented in Table I. Mostly, the Table includes only discharges of duration sufficient to

TABLE I. LISTING OF DISCHARGES FOR WHICH THE ION TEMPERATURE HAS BEEN MEASURED USING NEUTRON SPECTROMETRY

Group-Type	Pulse	B_T	I_p	n_e	\hat{T}_e	t_s-t_f	\hat{T}_i (neut)	
1 - Ω	2852	3.4	3.3	5.0	3.7	45-51	$2.32 \pm .33$	
	2854	3.4	3.4	5.3		45-51	$2.39 \pm .41$	
	2855	3.4	3.4				$2.97 \pm .41$	
	2856	3.4	3.3	5.5	3.4	45-51	$3.05 \pm .49$	
	2857	3.4	3.4	5.5		45-51	$3.65 \pm .64$	
	2858	3.4	3.4	5.4	3.4	45-51	$3.19 \pm .52$	
			3.4	3.4	5.3	3.5		$2.93 \pm .20$
2 - Ω	3048	3.4	3.6	5.6	3.8	44-51	$3.92 \pm .67$	
	3049	3.4	3.6	5.6	3.8		$3.32 \pm .49$	
	3050	3.4	3.6		3.7	45-51	$3.23 \pm .49$	
	3051	3.4	3.6	5.8	3.5		$2.26 \pm .34$	
	3052	3.4	3.5	5.9	3.5	45-50	$2.59 \pm .42$	
			3.4	3.6	5.7	3.7		$3.06 \pm .22$
3 - Ω	3905	3.4	3.5	3.2	3.3		$2.16 \pm .44$	
	3906	3.4	3.5	3.6	3.0	46-51	$2.25 \pm .48$	
	3907	3.4	3.5	4.0	3.0	47-61	$2.11 \pm .42$	
	3908	3.4	3.5	3.8	2.8	48-51	$2.28 \pm .42$	
			3.4	3.5	3.6	3.0		$2.20 \pm .22$
4 - Ω	4592	3.4	4.0	4.2	2.8	47-52	$2.37 \pm .45$	
	4593	3.4	4.0	4.4	2.7	47-51	$2.11 \pm .30$	
	4595	3.4	4.0	3.8		48-51	$2.45 \pm .37$	
			3.4	4.0	4.1	2.7		$2.31 \pm .22$
			3.4	4.0	3.6	3.7		$3.25 \pm .55$
5 - Ω	4782	3.4	4.0	3.6	3.7		$3.25 \pm .55$	
	4783	3.4	4.0	3.4	3.5	47-50	$3.13 \pm .54$	
	4784	3.4	4.0	3.2		46-51	$3.33 \pm .54$	
	4788	3.4	4.0	3.7	3.3	47-51	$2.55 \pm .41$	
	4791	3.4	4.0	3.8	3.2	47-51	$2.42 \pm .39$	
			3.4	4.0	3.5	3.4		$2.94 \pm .22$
6 - Ω	5349	3.4	4.6	3.9	3.2	46-50	$2.08 \pm .33$	
	5350	3.4	4.8	3.9	4.6	46-49	$2.20 \pm .35$	
			3.4	4.7	3.9	3.9		$2.14 \pm .25$

(to be continued overleaf)

TABLE I (cont.)

Group-Type	Pulse	B_T	I_p	n_e	\hat{T}_e	t_s-t_f	\hat{T}_i (neut)	
7 - RF	6777	3.4	3.8	3.9	3.8	44-50	$3.90 \pm .45$	
	6962	2.8	3.0	2.0	3.3			
	6964	2.8	3.0	2.0	3.3			
	6965	2.8	3.0	2.1	3.3			
8 - Ω	6966	2.8	3.0	2.2	3.3			
	6967	2.8	3.0	2.2	3.3			
	6968	2.8	3.0	2.2	3.3			
	6969	2.8	3.0	2.3	3.3			
			2.8	3.0	2.1	3.3	46-52	$3.06 \pm .36$
			2.8	3.0	2.1	3.3		
14 - RF	7163	3.4	3.0	4.0	3.7	45-49	$4.10 \pm .60$	
	7165	3.4	3.0	3.6	4.2	45-49	$5.00 \pm .77$	
	7168	3.4	3.0	4.0	3.8	45-50	$5.25 \pm .71$	
	7170	3.4	3.0	4.2	3.6	45-48	$4.25 \pm .53$	
	7171	3.4	3.0	3.8	3.5	45-49	$3.15 \pm .50$	
	7179	3.4	3.0	4.1	3.2	45-49	$3.87 \pm .71$	
	7180	3.4	3.0	4.0	3.5	45-48	$3.75 \pm .56$	
			3.4	3.0	4.0	3.7		$4.00 \pm .25$
15 - Ω	7283	3.4	4.0	3.9	2.9	46-53	$3.54 \pm .55$	
	7284	3.4	4.5	3.9	3.0	45-53	$3.58 \pm .50$	
	7285	3.4	4.5	4.8	2.8	45-52	$2.93 \pm .36$	
	7287	3.4	5.0	5.2	2.7	45-53	$2.99 \pm .30$	
	7293	3.4	5.0	5.1	2.8	45-52	$2.64 \pm .30$	
			3.4	4.6	4.6	2.8		$2.99 \pm .16$
16 - Ω	7607	2.8	3.0	2.5	3.3			
	7608	2.8	3.0	2.5	3.3			
	7611	2.8	3.0		3.3			
	7612	2.8	3.0		3.4			
	7613	2.8	3.0		3.4			
			2.8	3.0	2.5	3.3	46-52	$2.37 \pm .26$

- Notes: (i) B_T in T; I_p in MA; n_e in $10^{19} m^{-3}$; \hat{T}_e, \hat{T}_i in keV.
(ii) Pulses 5349, 5350 did not reach equilibrium conditions.
(iii) $t_s - t_f$ indicates start and finish times (in seconds) for the data acquisition; the discharge is initiated at $t = 40$ s.

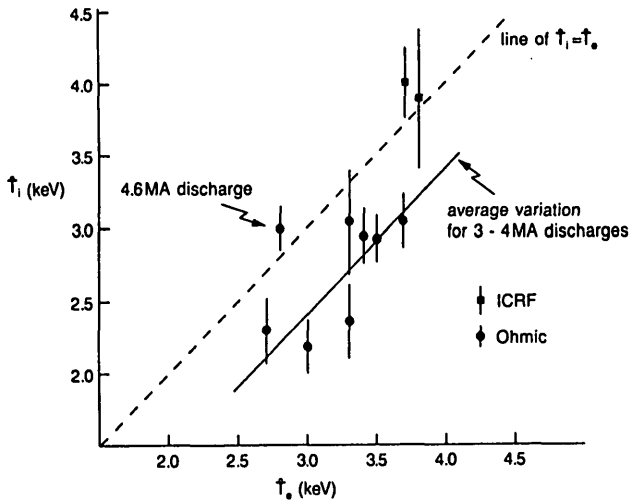


FIG. 1. Variations of \hat{T}_i with \hat{T}_e for the discharges studied. Electron temperature data have $\pm 10\%$ normalization uncertainty. Points are plotted only for those discharges for which equilibrium conditions were obtained.

ensure steady state equilibrium between electron and ion temperatures, although Group 6 is a notable exception.

Since neutron spectrometry cannot yet be regarded as an established method of measuring ion temperatures, it is necessary to inspect the data carefully for consistency with other measurements. A comparison of ion temperature measurements has shown that the agreement with results from the Neutral Particle Analysis technique [6] and from the X-ray crystal spectrometer [7] is very good over the temperature range from 2 to 5 keV, this latter value being achieved by using hydrogen neutral beam heating. To be useful in establishing a density ratio temperature dependence, the ion temperatures should be accurate to about 5% – a challenging requirement. Notwithstanding the relative precision of the different diagnostic methods, the neutron spectrometer temperature is strongly preferred for density ratio determinations because it is

TABLE II. DEUTERIUM ION TO ELECTRON DENSITY RATIOS AND CORRESPONDING Z_{eff} VALUES AVERAGED OVER GROUPS OF SIMILAR DISCHARGES

Group-Type	\hat{n}_d/\hat{n}_e	h/h+d	$^3\text{He}/n_e$	\hat{n}_C/\hat{n}_e (%)	Z_{eff}	Z_{eff} (VB)	Z_{eff} (Res)
1 - Ω	$0.50 \pm .08$	0.05	-	5.9 ± 1.1	3.9 ± 0.4	4.1 ± 0.7	5.0
2 - Ω	$0.42 \pm .08$	0.05	-	7.1 ± 1.1	4.4 ± 0.4	3.6 ± 0.6	5.2
3 - Ω	$0.77 \pm .15$	0.03	-	2.5 ± 2.0	2.5 ± 0.8	4.0 ± 0.6	3.5
4 - Ω	$0.60 \pm .14$	0.03	-	4.7 ± 1.8	3.4 ± 0.8	3.1 ± 0.5	3.0
5 - Ω	$0.46 \pm .07$	0.03	-	6.7 ± 0.8	4.2 ± 0.3	3.9 ± 0.6	4.4
6 - Ω	$0.71 \pm .15$	0.10	-	2.5 ± 2.0	2.5 ± 0.8	3.4 ± 0.6	5.5
7 - RF	$0.40 \pm .11$	0.05	0.025	6.9 ± 1.4	4.4 ± 0.6	3.2 ± 0.5	3.8
8 - Ω	$0.31 \pm .07$	0.05	-	8.5 ± 0.9	5.0 ± 0.4	3.6 ± 0.6	4.9
14 - RF	$0.35 \pm .05$	0.08	0.025	7.3 ± 0.6	4.5 ± 0.3	2.9 ± 0.5	4.7
15 - Ω	$0.34 \pm .04$	0.21	-	7.2 ± 0.5	4.4 ± 0.3	2.6 ± 0.5	4.1
16 - Ω	$0.52 \pm .09$	0.03	-	5.8 ± 1.2	3.8 ± 0.5	3.0 ± 0.5	4.7
Average (less Group 6) ^a				5.9	3.9	3.4	4.4

Systematic uncertainty in \hat{n}_d/\hat{n}_e has been ignored; a $\pm 10\%$ uncertainty gives an additional uncertainty in Z_{eff} of ± 0.5 at $Z_{eff} = 4$.

Impurities: H/H+D – measured
 C:O ratio = 5:1, provides balance
 Cl – 0.05%
 Ni – 0.05%

^a Group 6 did not achieve thermal equilibrium.

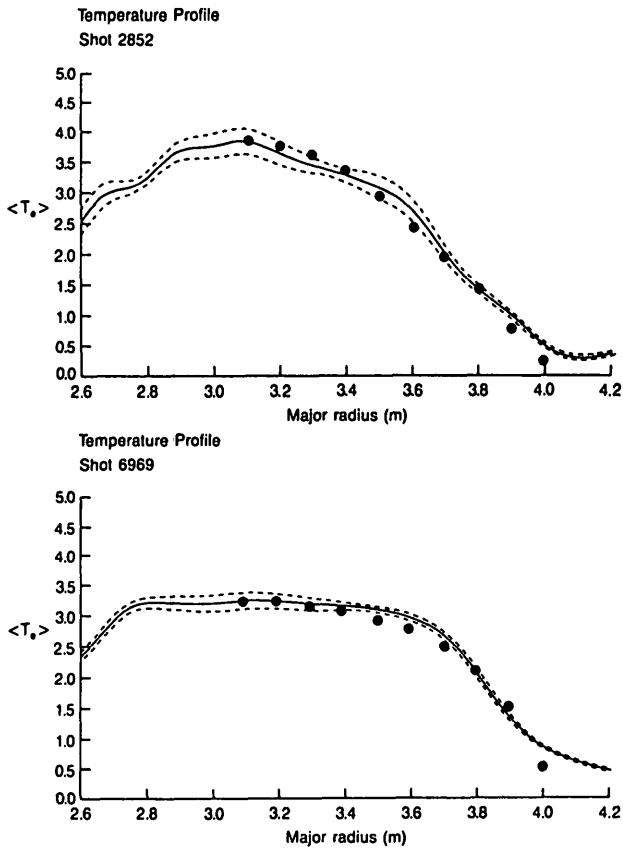


FIG. 2. Time averaged electron temperature profiles. The curves show the experimental measurements and confidence levels whilst the points show the fit of the assumed functional form to the data.

mostly sensitive to the high energy tail of the deuterium ion energy distribution which, after weighting by the d-d fusion reaction cross-section, is also responsible for the major part of the neutron emission strength. In this specific context all other techniques for measuring ion temperatures are less appropriate and may be subject to problems of interpretation. However, the fact that the three measurement techniques provide similar values of \hat{T}_i can be taken as good evidence that the energy distribution of the bulk plasma deuterium ions is essentially Maxwellian.

A comparison of the neutron ion temperature \hat{T}_i , with the central electron temperature, \hat{T}_e , is shown in Fig. 1. The essential observation is that \hat{T}_i increases with \hat{T}_e , lagging by about 0.6 keV for ohmically heated plasmas. However, remembering the $\pm 10\%$ normalization uncertainty associated with the electron temperature data and the $\pm 5\%$ uncertainty for the ion temperature data, it is clearly impossible to draw firm conclusions regarding the temperature differences.

5. THE DILUTION FACTORS

Given reliable \hat{T}_i data, the neutron emission strength from the fission chambers, the line integrated electron density from the 2 mm interferometer [8], the electron density radial dependence from the Far Infrared Interferometer [9], the electron temperature radial dependence from the Electron Cyclotron Emission diagnostic [10] and the assumption that ion and electron radial dependencies are the same, then the density ratio \hat{n}_d/\hat{n}_e can be determined (see Table II). The expression assumed for the plasma reactivity $\langle\sigma v\rangle$ is that of Peres (11).

The radial dependence of the electron temperature is much stronger than that of the electron density and therefore merits careful investigation. The ECE diagnostic [10] provides temperature profiles at very frequent intervals so as to exhibit the effect due to sawtooth oscillations. For present purposes it was appropriate to derive a profile which was the average in time over the interval during which the neutron energy spectra were accumulated, thereby suppressing all sawtooth effects. Because JET plasmas are D-shaped, a functional form for the spatial dependence of electron temperature was adopted:

$$T_e(R,Z) = T_{e0} \Psi^p(R,Z)$$

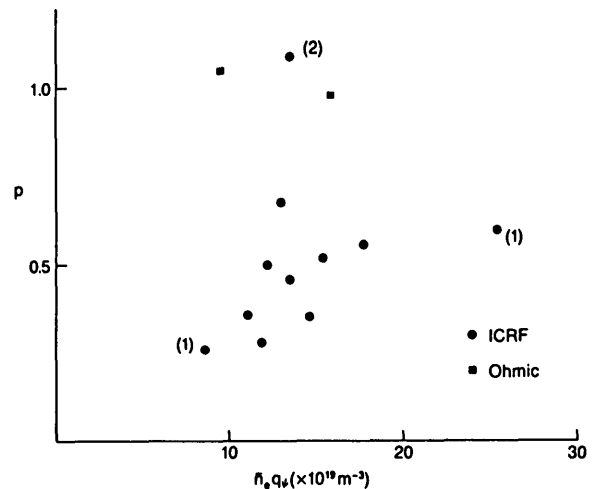


FIG. 3. Peaking factor for the electron temperature radial profile, averaged over the time interval for the ion temperature measurement.

- (1) Additional points (i.e. no neutron spectra).
- (2) Very early data for which ECE profiles are not as reliable as for later data.

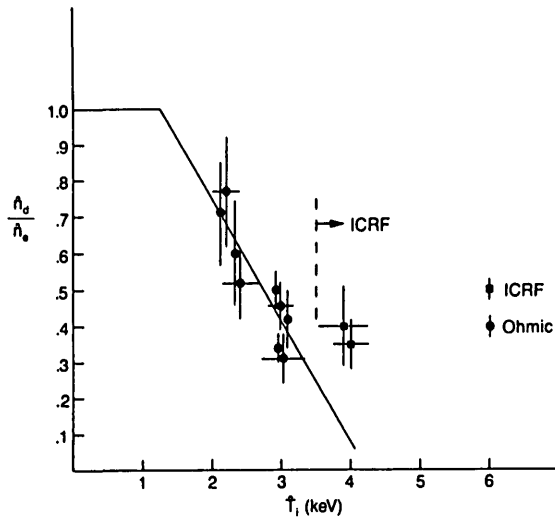


FIG. 4. Variation of \hat{n}_d/\hat{n}_e with central ion temperature for Ohmic and ICRF (^3He) heating. ICRF data points not adjusted for ^3He addition. The line is fitted to the Ohmic points only.

where Ψ is a suitable parameterization for the magnetic flux surfaces valid for low β plasmas. For circular plasmas, $T_e(R, Z) \approx T_{e0}(1 - r^2/a^2)^{2p}$, where a is the limiter radius. Values for the peaking parameter, p , were obtained by equating the functional form to the measured radial profile at $R = R_0$ ($R_0 \approx 3.05$ m) and $R = 3.80$ m, as illustrated in Fig. 2 for two ohmically heated discharges. Peaking factors for all data groups of interest are plotted in Fig. 3 as a function of $\bar{n}_e q_\Psi$, where q_Ψ is the plasma safety factor. It is interesting to note that the peaking values for the ICRF heated discharges are double those for Ohmic discharges. It should be recognized that flux surfaces are actually contours of constant pressure so that to assume density, n_e , and temperature, T_e , are separately constant may not be entirely correct.

The density ratios from Table II are shown in Fig. 4, plotted as a function of \hat{T}_i . A very strong temperature dependence is seen, with \hat{n}_d/\hat{n}_e falling from 75% at 2 keV to 40% at 3 keV. This result explains the low neutron yields obtained from JET for the ostensible plasma parameters achieved.

It should be appreciated that part of the decrease of the density ratio with \hat{T}_i is self-inflicted owing to the practice of glow discharge cleaning with CH_4 , which leads to high hydrogen concentrations in subsequent discharges, and to the use of ^3He as minority ion species for ICRF heating. For d-t operation neither circumstance should apply.

Finally, we note that the uncertainties provided in Table II are derived solely from the statistical errors in the \hat{T}_i measurement. There are also errors of a systematic nature which cannot be neglected. These include the normalization error in the \hat{T}_i data ($\pm 5\%$) and the error in the central electron density ($\pm 5\%$). In addition, the minority ^3He density is quite uncertain (factor of two) and the H density in the plasma centre can be inferred only to $\pm 50\%$. The most important source of uncertainty, however, derives from our lack of knowledge concerning the ion temperature profile, which almost certainly differs from that for the electron temperature, contrary to assumption. Work in progress has provided tentative indications that the ion temperature profile may be more sharply peaked than the electron temperature profile for the very high plasma current discharges (5 MA). If we adopt a $\pm 50\%$ uncertainty in the peaking factor for the ion temperature profile, then there will be a $\pm 25\%$ uncertainty in the normalization of the \hat{n}_d/\hat{n}_e results. This does not affect the observed \hat{T}_i dependence. Indeed, for \hat{n}_d/\hat{n}_e to be independent of \hat{T}_i , the peaking factor for \hat{T}_i would have to increase by a scarcely credible factor of four as \hat{T}_i rises from 2 to 3 keV.

6. DETERMINATION OF Z_{eff}

It is customary to determine Z_{eff} directly from bremsstrahlung measurements in the visible [12] and X-ray regions, to identify the various impurities in the plasma and thus to deduce the \hat{n}_d/\hat{n}_e ratio. However, having measured the \hat{n}_d/\hat{n}_e ratios, we are now in a position to reverse the procedure. The resulting Z_{eff} is strictly appropriate to the central region of the plasma, whereas the bremsstrahlung measurements are line of sight averages.

Very little spectroscopic information is available for the discharges listed in Table I so we adopt the heavy impurity concentrations of 0.05% Cl and 0.05% Ni as being typical of all. The most important impurities are C and O, which are shown to be present in the proportions 5 : 1 by the active charge exchange recombination spectrometry measurements [13]; typical concentrations for ohmically heated plasmas are 5.5% C and 1.0% O. As these observations were not available for the discharges of present interest, we assume the balance of the electron supply after all other sources are taken into account is attributable to C and O in the stated proportions.

For ICRF heated discharges it is assumed that 2.5% ^3He is added to the plasma (i.e. 5% increase in n_e). We

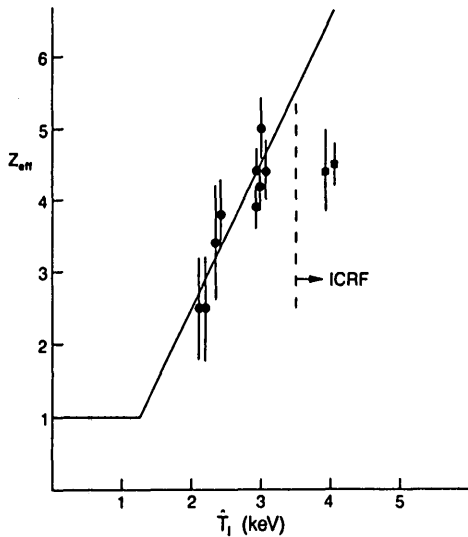


FIG. 5. Variation of Z_{eff} with central ion temperature. The solid line corresponds to that in Fig. 4.

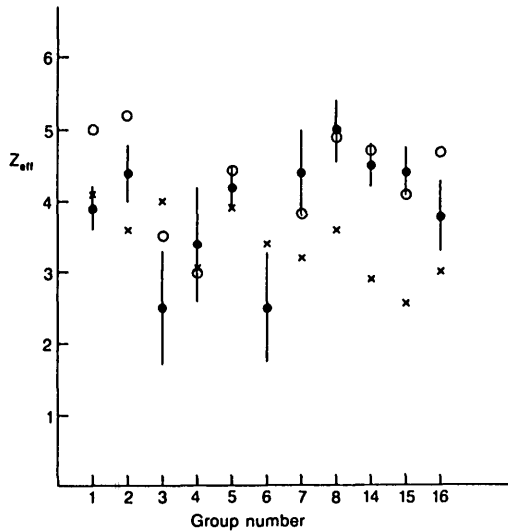


FIG. 6. Comparison of Z_{eff} values obtained from neutron measurements with values from axial resistivity and visible bremsstrahlung measurements. Φ : neutrons, \times : visible bremsstrahlung, \circ : axial resistivity. Each set of data has an associated normalization error which may be as large as $\pm 25\%$.

have measured the deuterium concentrations. Finally, the hydrogen/deuterium ratio is provided by the neutral particle analysis diagnostic. The resulting values for Z_{eff} are listed in Table II, together with the visible bremsstrahlung data and values calculated from the axial plasma resistivity [14] on the assumption that $q_0 = 0.8$. In Fig. 5, the Z_{eff} values deduced from the density ratios are plotted as a function of \hat{T}_i , a clear increase with \hat{T}_i being shown.

The 'neutron' Z_{eff} values are displayed in Fig. 6 by group number for comparison with Z_{eff} from visible bremsstrahlung measurements and axial resistivity calculations. The bremsstrahlung measurements represent volume averaged Z_{eff} values; to obtain the required axial values an upwards adjustment (of perhaps 25%) should be made. It is concluded that the three Z_{eff} determinations are in fair agreement, bearing in mind their appreciable associated systematic as well as statistical uncertainties.

7. DISCUSSION

The use of neutrons for diagnostic purposes has several advantages. The measurements involve just those reactions which are at the heart of the quest for power from nuclear fusion, they are not troubled by the complexities which plague measurements on low energy radiation and neutral particle emission and, above all, they become easier as the neutron emission strength rises. The measurement of neutron intensity is accurate and troublefree whilst the neutron energy spectra are easy to interpret for Maxwellian plasmas.

The essential experimental finding is that the high temperature ohmically heated plasmas ($\hat{T}_i \approx 3$ keV) are heavily contaminated with impurities (known from other sources to be mainly carbon and oxygen). In addition, it appears that the impurity level at lower temperatures (2–2.5 keV) is much lower. Because of the rather large statistical uncertainties associated with the low temperature data, it is not possible to be emphatic on this point but it should be noted that the requirement that neutron yields be high for the temperature measurement to be possible means that results cannot be obtained for low temperature plasmas with high impurity levels. Thus, for the Ohmic discharges studied, a correlation between impurity level and ion temperature is indicated but a direct ion temperature dependence is not claimed. Indeed, the observation that the addition of ICRF heating raises the ion temperature without significantly changing the impurity level demonstrates that it is the electron temperature rather than the ion temperature which may be determined by Z_{eff} .

A temperature dependence of the impurity level might be expected on the grounds that the effectiveness of Ohmic heating is directly proportional to Z_{eff} . For the high current discharges studied, the observation of sawtoothing is evidence for the safety factor q being almost unity in the central region of the plasma and hence the central current density (and Ohmic heating

power) is nearly independent of the total plasma current. Consequently, the relationship between the central ion temperature and the impurity level is not expected to be affected by the plasma current. Further, the observation that the increase in ion temperature due to the addition of ICRF heating is not correlated with an increase of the impurity level demonstrates that the ion temperature does not directly control the impurity level in the plasma. This finding is fully in accord with the general understanding that the impurity level in the plasma is determined by the plasma boundary conditions during the early stages of a discharge and is thus essentially decoupled from the conditions in the plasma centre at a later time.

REFERENCES

- [1] SWINHOE, M.T., JARVIS, O.N., Nucl. Instrum. Methods Phys. Res. **221** (1984) 460.
- [2] JARVIS, O.N., KÄLLNE, J., SADLER, G., VAN BELLE, P., HONE, M., MERLO, V., LEES, E.W., SWINHOE, M.T., TALBOT, A.R., ARMITAGE, B.H., Further Calibrations of the Time Resolved Neutron Yield Monitor (KN1), Rep. JET-IR(85) 06, JET Joint Undertaking, Abingdon, Oxfordshire (1985).
- [3] JARVIS, O.N., GORINI, G., HONE, M., KÄLLNE, J., MERLO, V., SADLER, G., VAN BELLE, P., Rev. Sci. Instrum. **57** (1986) 1717.
- [4] SADLER, G., VAN BELLE, P., HONE, M., JARVIS, O.N., KÄLLNE, J., MARTIN, G., MERLO, V., in Controlled Fusion and Plasma Heating (Proc. 13th Europ. Conf. Schliersee, 1986), Vol. 10C, Part I, European Physical Society (1986) 105.
- [5] GORINI, G., HONE, M., JARVIS, O.N., KÄLLNE, J., MERLO, V., SADLER, G., VAN BELLE, P., in Basic Physical Processes of Toroidal Fusion Plasmas (Proc. Course and Workshop Varenna, 1985), Vol. 1, Rep. EUR-10418 EN, CEC (1986) 133.
- [6] BRACCO, G., CORTI, S., ZANZA, V., BARTIROMO, R., BITTI, G., et al., First Results from JET Neutral Particle Analyser (NPA), Rep. JET-IR(84) 04, JET Joint Undertaking, Abingdon, Oxfordshire (1984).
- [7] GIANELLA, R., BOMBARDA, F., KÄLLNE, E., PANACCIONE, L., TALLENTS, G., Bull. Am. Phys. Soc. **31** (1986) 1590.
- [8] FESSEY, J.A., GOWERS, C.W., HUGENHOLTZ, C.A.J., SLAVIN, K., J. Phys., E: Sci. Instrum. **20** (1987) 169.
- [9] BRAITHWAITE, G., BULLIARD, A., BRUNEAU, J-L., HANCOCK, J., MAGYAR, G., et al., The Multichannel Far Infrared Interferometer (KG1) on JET, Rep. JET-IR(85)06, JET Joint Undertaking, Abingdon, Oxfordshire (1985).
- [10] COSTLEY, A.E., BARKER, E.A.M., BRUSATI, M., BARTLETT, D.V., CAMPBELL, D.J., et al., in Controlled Fusion and Plasma Physics (Proc. 12th Europ. Conf. Budapest, 1985), Vol. 9F, Part I, European Physical Society (1985) 227.
- [11] PERES, A., J. Appl. Phys. **50** (1979) 5569.
- [12] BEHRINGER, K.H., CAROLAN, P.G., DENNE, B., DECKER, G., ENGELHARDT, W., et al., Nucl. Fusion **26** (1986) 751.
- [13] HORTON, L.D., VON HELLERMAN, M.G., SUMMERS, H.P., PEACOCK, N.J., Bull. Am. Phys. Soc. **31** (1986) 1590.
- [14] CHRISTIANSEN, J.P., Integrated Analysis of Data for JET, Rep. JET-R(86)04, JET Joint Undertaking, Abingdon, Oxfordshire (1986).

(Manuscript received 24 March 1987
Final manuscript received 6 July 1987)